Dyn Games Appl (2012) 2:177–194
DOI 10.1007/s13235-012-0042-y

The Spatialized, Continuous-Valued Battle of the Sexes

Ramón Alonso-Sanz

Published online: 28 February 2012

Abstract The dynamics of a spatial, continuous-valued formulation of the iterated battle of the sexes is assessed in this work. The game is played in the cellular automaton manner, i.e., with local and synchronous interaction. The effects of probabilistic updating and memory of past encounters are also taken into account. With deterministic updating, the spatial structure enables the emergence of coordination clusters, leading to the mean payoffs per encounter to values that are accessible only in the cooperative two-person game scenario, which constitutes a notable case of self-organization. With probabilistic updating of choices, both kinds of player tend to reach a full coordination absorbing steady state in the long term. As a general rule, short-term memory of past iterations does not qualitatively alter the ahistoric dynamics. Unlimited trailing memory induces an inertial effect that alters the dynamics to a larger extent, particularly in the probabilistic updating scenario, in which case unlimited trailing memory fully inhibits the dynamics.

Keywords Battle of the sexes · Spatial · Continuous · Memory

1 Introduction

The so called *battle of the sexes* (BOS for short) is a simple example of a two-person asymmetric game [13, 17]. In this game, the preferences of a conventional couple are assumed to fit the traditional stereotypes: the male prefers to attend a *F*ootball match, whereas the female prefers to attend a *B*allet performance. Both players (which are treated symmetrically), decide in the hope of getting together, so that their payoff matrices are given in the far left panel of Table 1, with rewards $R > r > 0$. There are both coordination and conflict elements in the BOS game [16]. While both players want to go out together, the *conflict* element is present because their preferred activities differ, and the *coordination* element is present because they may end up going to different events. Thus, in the absence of preplay

R. Alonso-Sanz (✉)
ETSI Agrónomos (Estadística, GSC), Universidad Politécnica de Madrid, C.Universitaria, 28040, Madrid, Spain
e-mail: ramon.alonso@upm.es

Table 1 The payoff matrices (left), reaction correspondences (center) and payoff region (right) in the *battle of the sexes* game

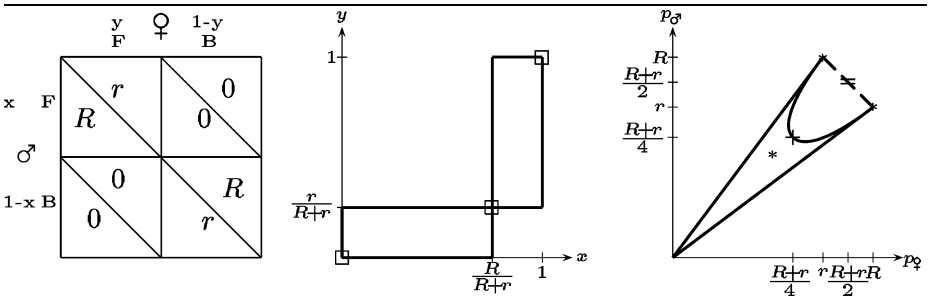

communication it is natural to expect that coordination failure (of ending up in one of the inefficient outcomes) will occur frequently.

The expected payoffs (p) in the BOS game, using uncorrelated mixed probabilistic strategies $(x, 1-x)$ and $(y, 1-y)$ are

$$p_{♂}(x; y) = (x, 1-x)\begin{pmatrix} R & 0 \\ 0 & r \end{pmatrix}\begin{pmatrix} y \\ 1-y \end{pmatrix} = \big((R+r)y - r\big)x + r(1-y), \tag{1}$$

$$p_{♀}(y; x) = (x, 1-x)\begin{pmatrix} r & 0 \\ 0 & R \end{pmatrix}\begin{pmatrix} y \\ 1-y \end{pmatrix} = \big((R+r)x - R\big)y + R(1-x). \tag{2}$$

The pair of strategies $((x, 1-x), (y, 1-y))$, are in Nash equilibrium if x is a best response to y and y is a best response to x. Formally: $p_A(x, y) \geq p_A(z, y)$, and $p_B(x, y) \geq p_B(x, z)$, $\forall z$. Nash equilibria are shown with points where the two player's correspondences agree, i.e. cross, in the reaction correspondence graphs. Thus, according to the reaction correspondences given in Table 1, the pairs of strategies in Nash equilibrium are the pure $(0, 0)$ and $(1, 1)$, and the mixed $(x^* = R/(R+r), y^* = r/(R+r))$ ones. In the latter case, $p_{♂}(x^*, y^*) = p_{♀}(x^*, y^*) = rR/(R+r) < r < R$.

Both players get the same payoff if $y = 1-x$, in which case, $p = (R+r)(1-x)x$. This egalitarian payoff is maximum when $x = y = 1/2$, with $p^+ = (R+r)/4$, the point marked $+$ in the far right panel of Table 1. Thus, the set of payoffs which can be obtained by both players (or payoff region) is closed by the parabola passing by (R, r), (r, R), and (p^+, p^+), as shown in the payoff region panel of Table 1.

In a broader game scenario, a probability distribution $A = (a_{ij})$ assigns probability to every combination of player choices, so $A = \left(\begin{smallmatrix} a_{11} & a_{12} \\ a_{21} & a_{22} \end{smallmatrix}\right)$ in 2×2 games [21]. Thus, the expected payoffs in the BOS are $\begin{smallmatrix} p_{♂} = a_{11}R + a_{22}r \\ p_{♀} = a_{11}r + a_{22}R \end{smallmatrix}$. The probability distribution (strategy) $A = (a_{ij})$ is in *correlated equilibrium* [8] if the players cannot gain by disobeying the signals given by the randomization device A. Thus, in the BOS game, $A = \left(\begin{smallmatrix} a & 0 \\ 0 & 1-a \end{smallmatrix}\right)$ is in correlated equilibrium, giving: $\begin{smallmatrix} p_{♂} = aR + (1-a)r \\ p_{♀} = ar + (1-a)R \end{smallmatrix}$, so that the payoff region limited by the parabola and the segment that joins (R, r) and (r, R) becomes accessible. In this scenario both players reach a maximum egalitarian payoff $p^= = (R+r)/2$ (the point marked $=$ in the payoff region of Table 1), with $a = 1/2$, i.e., fully discarding the mutually inconvenient FB and BF combinations and adopting FF and BB with equal probability.

The paper is structured as follows. In Sect. 2 the spatial cellular automaton BOS game is defined and the case of deterministic updating of choices, via pure imitation of the best

rewarded player, is studied. In order to contextualize the continuous-valued scenario studied in this work, Sect. 2 briefly deals with the binary choice model in its first subsection. Probabilistic updating of choices is studied in Sect. 3, whereas the effect of taking into consideration previous iterations, not only the last one, is analyzed in Sect. 4. Conclusions and potential ways of further studies are discussed in Sect. 5.

2 The Spatialized BOS: Deterministic Updating

In the spatial version of the BOS cellular automaton we dealt with, each player occupies a site (i, j) in a two-dimensional $N \times N$ lattice. We will consider that *males* and *females* alternate in the site occupation, so that in the chessboard form shown in the far left panel of Table 2, every player is surrounded by four partners (♀-♂, ♂-♀), and four mates (♀-♀, ♂-♂).

In a CA-like implementation, in each generation (T) every player plays with his four adjacent partners, so that the payoff of a given individual $(p_{i,j}^{(T)})$, is the sum over these four interactions. In the next generation, every player will adopt the choice $(d_{i,j}^{(T)})$ of his nearest-neighbor mate (including himself) that received the highest payoff. In case of a tie, the player maintains his choice.

All the simulations in this work are run in a 100×100 lattice with periodic boundary conditions. The even side size lattice fixed makes sure that the players in the borders are in the regular conditions regarding mate and partner neighborhood.

2.1 Binary Strategies

Figure 1 deals with the case of binary choices [4], or *crisp* degrees, thus both x and y are either 0.0 or 1.0. The football frequency and mean payoff per encounter (p) in a $(R = 5, r = 1)$ BOS cellular automaton starting from a random initial configuration of binary choices is shown in the left panel of Fig. 1. Initially, as a result of the random assignment of choices, the F-frequencies (and that of B) are 0.5, and the mean payoffs commence at the arithmetic mean of the payoff values, i.e., $p^+ = (R + r)/4 = 1.5$.

After the first round, both types of player drift to their preferred choice, and as consequence both payoffs plummet at $T = 2$. But immediately such a drift becomes moderated, and both p recover. In the long term the F-frequencies stabilize at values that are not off from the F-probabilities in the mixed equilibrium strategy of a two-person game: $x^* = R/(R + r) = 0.83$, $y^* = r/(R + r) = 0.17$.

The dotted curves in the left panel of Fig. 1 show the *theoretical* payoffs of both players in a two-person game with independent strategies using as probabilities the evolving frequencies, i.e., (1)–(2) rewritten as:

$$p_{♂}^{(T)} = \big((R + r)\overline{y} - r\big)\overline{x} + r(1 - \overline{y}),$$

$$p_{♀}^{(T)} = \big((R + r)\overline{x} - R\big)\overline{y} + R(1 - \overline{x}).$$

The actual mean payoffs of both kinds of player shown in Fig. 1 are over these *expected* values due to the spatial structure, which allows for the emergence of clusters of *agreement*, shown in the right panel of Fig. 1 as black (FF) and white (BB) regions with interfaces of disagreement among the clusters.

The study of spatial games was pioneered by Nowak and May [19, 20] with regards to the Prisoner's Dilemma (PD) [9]. They concluded in their original work that spatial structure (or

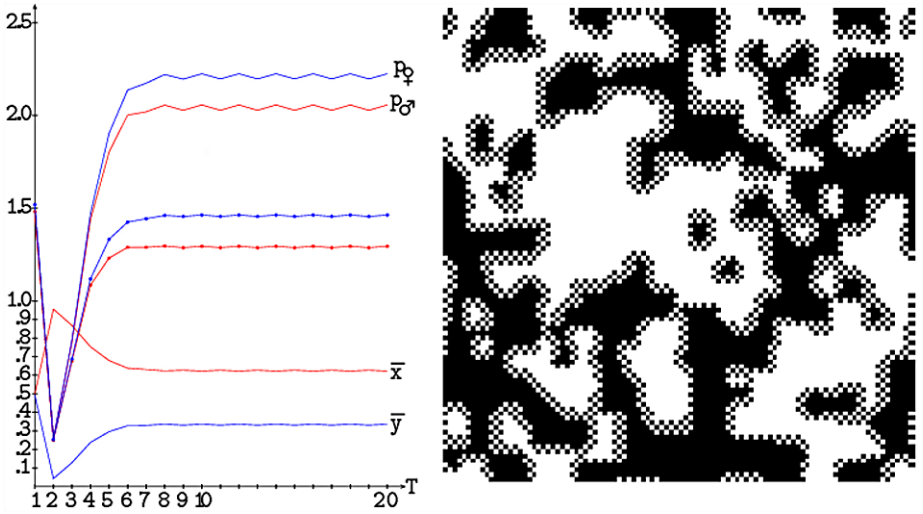

Fig. 1 *Left*: The Football choice frequencies $(\mathtt{x}, \mathtt{y})$ and mean payoffs per encounter $(\mathtt{p})$ in a simulation in the binary $(5, 1)$-BOS cellular automaton. *Right*: The pattern at $T = 20$: *Black/Blank* pixels indicate Football/Ballet choices

territoriality) can facilitate the survival of cooperators. Thus, the spatialized PD has proved to be a promising tool to explain how cooperation can hold out against the ever-present threat of exploitation. The notable case of self-organization in the BOS just presented appears as a novel example of the boosting effect induced by the spatial ordered structure, which allows the access to payoffs which are feasible only with correlated strategies in the two-person game.

Although involving $N \times N$ players, in the simulations considered in this study pairs of individuals interact in the 2-player, 2-strategy manner. Thus, we are not dealing with an n-person game, were all individuals of the group interact simultaneously. The n-person BOS game has been studied in [23, 24].

2.2 Continuous-Valued Strategies

As a natural extension of the binary model considered in 2.1, the strong 0-1 assumption underlying the model can be relaxed by allowing for *degrees* of choices in a continuous-valued scenario. Denoting by x and y the degrees of F choice of the ♂-player and the ♀-player, respectively, a consistent way to specify the payoff for values of x and y other than zero or one is to simply interpret the x and y in (1)–(2) as the F-degrees instead of probabilities. Consequently, the p-values become the actual payoffs in the continuous-valued context, instead of the expected payoffs in the probabilistic context.[1] Again, in each round or generation, every player plays with each of his/her four partner-neighbors and imitates the F-degree, instead of the binary choice, of the mate-neighborhood with the highest payoff. In case of a tie, i.e., several mate neighbors with the same maximum payoff, the average of the F-degrees corresponding to the best mate neighbors will be adopted.

In the initial scenario of Table 2, every player chooses his preferred choice, except a male in the central part of the lattice that chooses x at 0.5 level. As a result, the general

[1] We have studied such an approach dealing with the spatialized PD game [2, 7].

Table 2 The continuous-valued BOS cellular automaton. $R = 5$, $r = 1$

						$T=1$ x,y						$T=1$ $p_{♂},p_{♀}$						$T=2$ x,y						$T=2$ $p_{♂},p_{♀}$					
♂	♀	♂	♀	♂	♀	1	0	1	0	1	0	0	0	0	0	0	0	1	0	1	0	1	0	0	**2.5**	0	**2.5**	0	0
♀	♂	♀	♂	♀	♂	0	1	0	1	0	1	0	0	**2.5**	0	0	0	0	**0.5**	0	**0.5**	0	1	**2.5**	**2.0**	**7.5**	**2.0**	**2.5**	0
♂	♀	♂	♀	♂	♀	1	0	**0.5**	0	1	0	0	**2.5**	**2.0**	**2.5**	0	0	1	0	**0.5**	0	1	0	0	**7.5**	**2.0**	**7.5**	0	0
♀	♂	♀	♂	♀	♂	0	1	0	1	0	1	0	0	**2.5**	0	0	0	0	**0.5**	0	**0.5**	0	1	**2.5**	**2.0**	**7.5**	**2.0**	**2.5**	0
♂	♀	♂	♀	♂	♀	1	0	1	0	1	0	0	0	0	0	0	0	1	0	1	0	1	0	0	**2.5**	0	**2.5**	0	0
♀	♂	♀	♂	♀	♂	0	1	0	1	0	1	0	0	0	0	0	0	0	1	0	1	0	1	0	0	0	0	0	0

income is nil with the only exception arising from the ♂ $x = 0.5$ choice. This reports two units (assuming $r = 1$) to the initial $x = 0.5$ male, and fires the change to $x = 0.5$ of the four males connected with the initial ♂-$x = 0.5$ as indicated under $T = 2$ in Table 2. The change ♂-$x = 1.0$ to ♂-$x = 0.5$ advances in this way at every time-step, so that in this simple example every male player will choose $x = 0.5$ in the long term. Consequently, in the long term the male players will get two units and the female players will get ten units at every time-step.

Figure 2 deals with nine different simulations starting at random in what respect to the F-degrees in a $(R = 5, r = 1)$ continuous BOS cellular automaton. The figure shows up to $T = 200$ the evolution of the mean values across a 100×100 lattice of x and y, i.e., $\overline{x}$, $\overline{y}$, as well as of the payoffs. As a result of the random assignment of F-degrees, initially it is $\overline{x} = \overline{y} = 0.50$, $p_{♂} = p_{♀} = 1.5$ (as in the binary simulation just reported). After the first round, both types of player drift to their preferred degree in the continuous simulations of Fig. 2, and tend the *modulate* this initial trend in the following time-steps. Much as happened in the binary simulation in Fig. 1, but in a notably slower way. Please, note that the T-axis reaches 200 in Fig. 2, instead of 20 as in Fig. 1. In the simulation 3 of Fig. 2 both types of player reach an equalitary payoff close to 2.0. The simulations (2, 4, 5, 6) stabilize in fairly close payoffs, whereas in the remaining ones either the male type or the female type achieve higher payoffs. Thus, for example, in simulation 7.

Figure 3 shows the eight initial patterns and patterns at higher time-steps in the continuous (5, 1)-BOS CA simulation shown in the top-left panel 1 of Fig. 2. The fairly stable configuration is envisaged already at $T = 20$. It is to be noted that the black-regions tends to mask any not full F-degree, i.e., almost black albeit not full black.

3 Probabilistic Updating

In the probabilistic updating mechanism considered from this section, the individuals will play a F-degree with a probability proportional to its payoff among their mate neighbors.[2] Thus, denoting by $\mathcal{N}_i$ the mate neighborhood of the generic cell i, the probabilities that it is occupied by the F-degree of player j at time-step $T + 1$ is

$$P\left(x_i^{(T+1)} = x_j^{(T)}\right) = \frac{p_j^{(T)}}{\sum_{j\in\mathcal{N}_i} p_j^{(T)}}, \qquad P\left(y_i^{(T+1)} = y_j^{(T)}\right) = \frac{p_j^{(T)}}{\sum_{j\in\mathcal{N}_i} p_j^{(T)}}. \tag{3}$$

[2]The probabilistic updating mechanism has been implemented in the binary BOS context in [5].

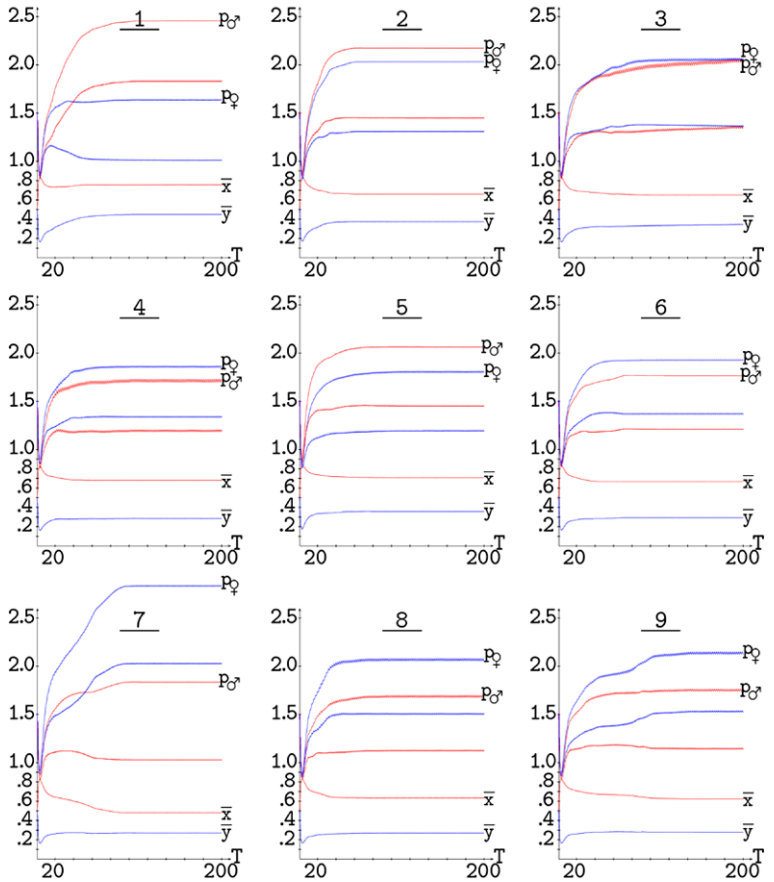

Fig. 2 The mean F-degrees $(\overline{x}, \overline{y})$ and payoffs per encounter (p) in nine simulations of the $(5, 1)$-BOS cellular automaton with deterministic updating. Ahistoric model

Figure 4 shows the evolution up to $T = 2000$ with probabilistic updating starting from the same nine initial scenarios of Fig. 2. After a comparatively short initial transition period, the F-degrees of both types of players tend to converge in fairly monotone manner, either increasing or decreasing. Thus, at variance with what happens in the deterministic simulations in Fig. 2, in the probabilistic simulations of Fig. 4 there is not any trend to stabilization in fairly close payoffs. On the contrary, with the only exception of simulation 8, the simulations reach a full coordination steady state before $T = 2000$, either to $(5, 1)$ or $(1, 5)$ payoffs, i.e., the crisp degrees (or pure equilibrium strategies) $(1, 1)$ and $(0, 0)$. This is so very soon in some simulations, e.g., 1 and 5, or later on, such as in 4 and 7. The simulation 8 reaches the $(5, 1)$ stable configuration by $T = 2900$.

Figure 4 shows the F-degree patterns at $T = 1000$ in the nine probabilistic simulations as insets. Simulations 1, 5 and 6 have already virtually reached their steady state, so that their corresponding patterns are either a full blank or a full black lattice. In the remaining simulations, with the only exception of simulation 8, the coordination clusters are already clearly formed at $T = 1000$, and indicate the long-term dynamics. Thus, (i) the full blank (BB) occupation in simulations 3, 4, 7 and 9 after the existence of a unique compact cluster

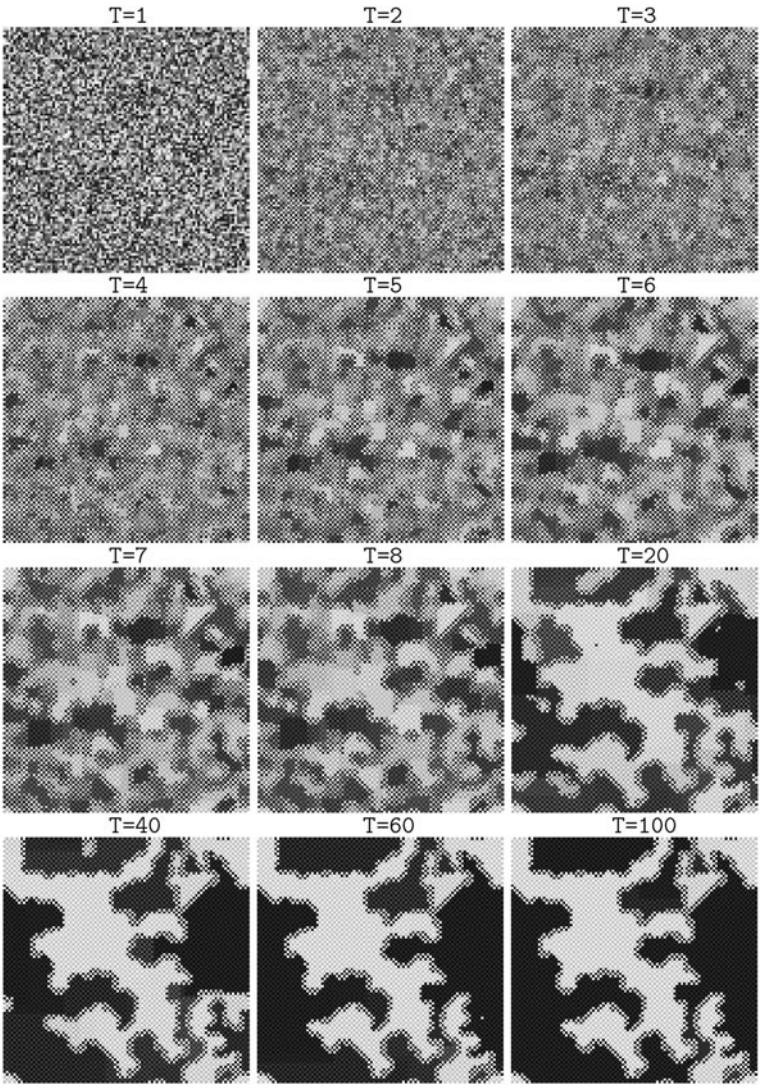

Fig. 3 Initial patterns and patterns at higher time-steps in the continuous $(5, 1)$-BOS CA simulation shown in the top-left panel 1 of Fig. 2. Increasing gray levels correspond to increasing F-degrees

of players with high F-degree, i.e., the black region, which tends to shrink until it disappears, and, the contrary case, (ii) the full black (FF) occupation in simulation 2 after the existence of a unique compact cluster of players with small F-degree, i.e., the blank region. The resiliency of simulation 8 maybe explained by the singular strip of BB players shown in Fig. 4, at $T = 1000$, which demands more time-steps for it to vanish.

Figure 5 shows some early F-degree patters patterns in the continuous $(5, 1)$-BOS CA with probabilistic updating simulation shown in the initial top-right panel 3 of Fig. 4. Some degree of nucleation may be envisaged as soon as at $T = 20$. This phenomenon is much

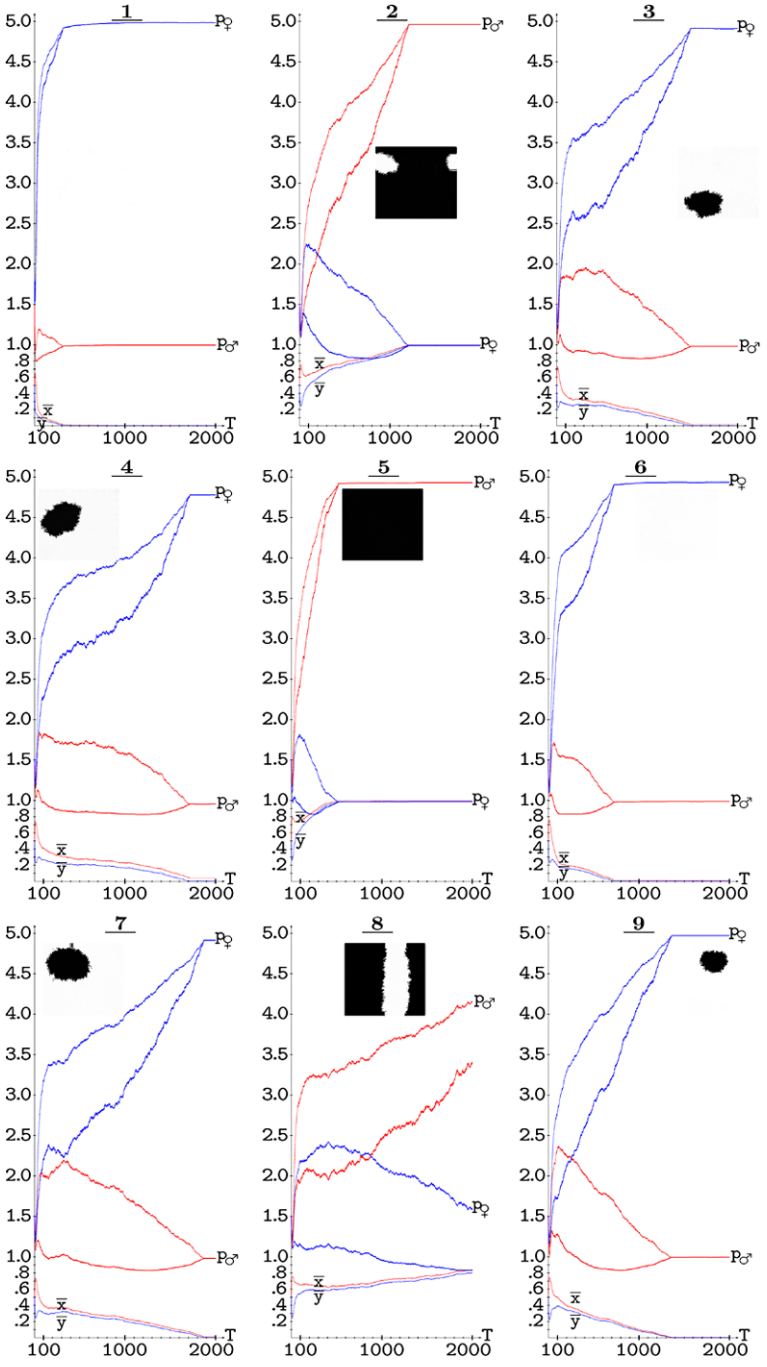

Fig. 4 The mean F-degrees $(\overline{x}, \overline{y})$ and payoffs per encounter $(\mathfrak{p})$ in nine simulations of the $(5, 1)$-BOS CA with probabilistic updating. Ahistoric model

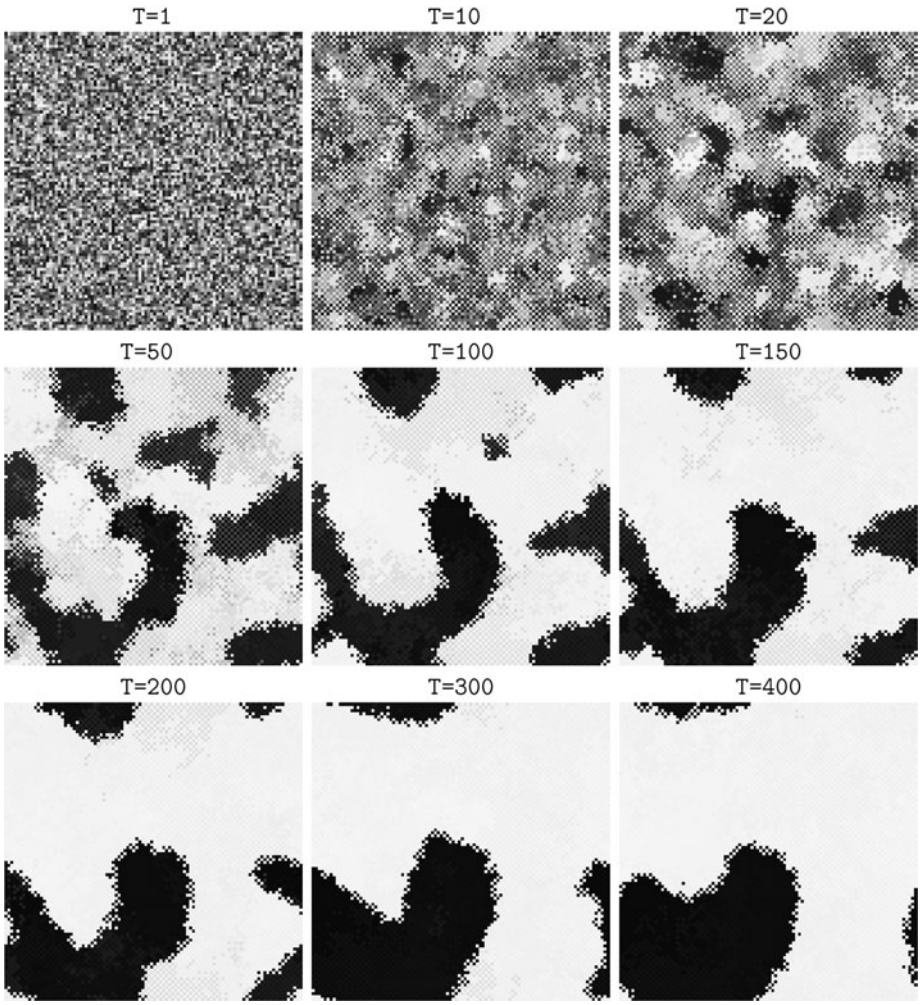

Fig. 5 Initial patterns and patterns at higher time-steps in the initial top-right simulation of Fig. 4. Increasing gray levels correspond to increasing F-degrees

evident at $T = 50$, and progresses in such a way that at $T = 400$ there is only a black *stain*, which is destined to disappear.

Let us point out here that in small lattices: (i) the nucleation phenomena just referred to are not found, (ii) coordination is hardly achieved at a perfect (or near perfect) level, (iii) the dynamics stabilize sooner compared to those in wider lattices. Thus for example, in nine simulations over a 20×20 lattice run up to $T = 400$, the dynamics is essentially stabilized before $T = 100$. Their mean payoffs ($p_{\male}$, $p_{\female}$) at $T = 400$ were found to be: $(0.99, 4.97)$, $(4.64, 0.93)$, $(4.21, 0.86)$, $(0.85, 4.25)$, $(4.77, 0.95)$, $(4.14, 0.84)$, $(3.84, 0.78)$, $(0.95, 4.76)$, $(4.83, 0.97)$.

All the simulations in Fig. 4 are implemented with the same sequence of random numbers (which we generated by means of the G05CAF NAG function). Different sequences of random numbers would produce different evolutions. Thus, for example the dynamics in

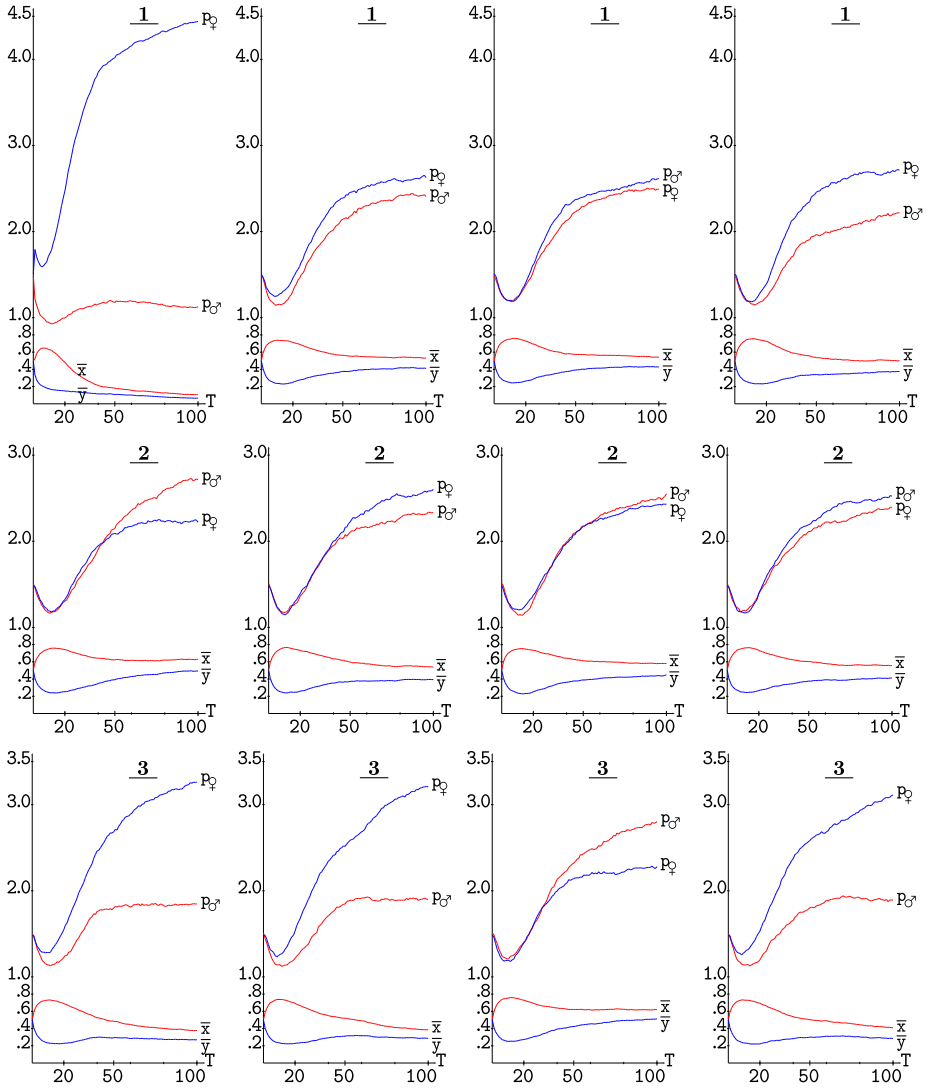

Fig. 6 The simulations 1 to 3 of Fig. 4 with four different sequences of random numbers

Fig. 6 correspond to the initial scenarios of simulations 1 to 3 in Fig. 4, but with four different randomization schemes, arising from different initialization seeds (we used G05CBF NAG function at this respect), being the far left one that corresponding to Fig. 4. The simulations in Fig. 6 are run just up to $T = 100$, which allows to appreciate the dynamics in the initial transition period. The four simulations 1 evolve with predominance of the female mean payoff, albeit the initial steep increase in the *original* (far left) simulation becomes much moderated in the alternative ones. In the case of simulations 2, it is remarkable that in two of the three alternative simulations the payoff predominance is inverted with respect to the *original* one: from that of $p_{\male}$ to that of $p_{\female}$. The alternative 2 simulation that preserves the $p_{\male}$ predominance makes it after an early swift (around $T = 30$) change in the

initial tendency. Two of the three alternative 3 simulations preserve the *original* p_{φ} predominance, whereas the other one inverts the p-predominance after a short period of equality. The remaining simulations in Fig. 4 have also been checked at this respect, i.e., with three alternative sequences of random numbers. The results of these simulations are qualitatively similar to those shown in Fig. 6. Thus, it can be concluded that, as a general rule, which one of the two possible steady states is reached in simulations with probabilistic updating in not fully determined by the initial distribution of F-degrees.

4 The BOS with Memory

As long as only the results from the last round are taken into account and the outcomes of previous rounds are neglected, the model considered up to now may be termed *ahistoric*, although it is not fully memoryless as there is a chain (or Markovian) mechanism inherent in it, so that previous results affect further outcomes.

In the *historic* model we consider in this section, after the time-step T, and for every cell i: (a) all the payoffs coming from the previous rounds are accumulated, giving $\pi_i^{(T)}(p_i^{(1)},\ldots,p_i^{(T)}) = p_i^{(T)} + \sum_{t=1}^{T-1} \alpha^{T-t} p_i^{(t)}$, and (b) players are featured by a summary of past F-degrees $(\chi_i^{(T)}, \upsilon_i^{(T)})$, not only the last one. Thus, for the male players

$$\chi_i^{(T)}\left(x_i^{(1)},\ldots,x_i^{(T)}\right) = \frac{x_i^{(T)} + \sum_{t=1}^{T-1} \alpha^{T-t} x_i^{(t)}}{1 + \sum_{t=1}^{T-1} \alpha^{T-t}} \equiv \frac{\omega_i^{(T)}}{\Omega^{(T)}}.$$

This geometric memory mechanism is *accumulative* in its demand for knowledge of past history: $\pi_i^{(T)} = \alpha\pi_i^{(T-1)} + p_i^{(T)}$, $\omega_i^{(T)} = \alpha\omega_i^{(T-1)} + x_i^{(T)}$.

The choice of the *memory factor* $0 \le \alpha \le 1$ simulates the remnant memory effect: the limit case $\alpha = 1$ corresponds to equally weighted records (*full* memory model), whereas $\alpha \ll 1$ intensifies the contribution of the most recent iterations and diminishes the contribution of the past ones (*short-term* memory); the choice $\alpha = 0$ leads to the ahistoric model. Table 3 shows the early dynamics with full memory in the initial scenario of Table 2.

We have studied the effect of the kind of memory implementation considered here[3] in the spatialized prisoner's dilemma game in various contexts [1–3, 6, 7], concluding that memory notably boosts cooperation.

Figure 7 shows the evolution up to $T = 1000$ of the F-degree and mean payoff per encounter in the nine initial scenarios of the deterministic (5, 1)-CA of Fig. 2 with $\alpha = 0.7$ memory. The F-degree patterns at $T = 1000$ are shown as insets in Fig. 7. Both Fig. 2 and Fig. 7 share a, let us say, common *shape*. But rather surprisingly, the dynamics with memory is stabilized notably later in four of the simulations (2, 5, 6 and 9). This contrasts with the same kind of comparison made in the binary scenario, in which case the length of the transition period is not significantly altered. Moreover, in the binary scenario memory does not significantly alters the levels of the (almost) stable F-degrees, whereas in the continuous case studied here, the F-degree plateaus, and consequently the p-plateaus no coincident with and without memory. Particularly in the case of delayed stabilization. Take for example the 2 simulation. The stabilized $(p_{\sigma}, p_{\varphi})$ payoffs are: (2.17, 2.01) without memory,

[3]Which differs from the usual memory implementation in spatial games, consisting of designing strategies which determine the next move of a player given the history (genome) of past moves [14, 15], whereas scores are treated in a Markovian way. Probabilistic simulations with genome-type memory are implemented in [12].

and (3.37, 1.31) with $\alpha = 0.7$ memory. By the way, none of these p-pairs is accessible in the independent players formulation of the game. Please, request that (1.50, 1.50) is the maximum possible equalitarian payoff in this context, and that the equation of the parabola closing the payoffs region is[4]: $3(p_{♂} - p_{♀})^2 - 16(p_{♂} + p_{♀}) + 48 = 0$, so that the maximum feasible male-payoff with fixed $p_{♀} = 1.31$ is the value on the parabola, $p_{♂} = 1.71$, which 3.37 notably exceeds.

Figure 8 shows the evolution up to $T = 1000$ of the F-degree and mean payoff per encounter in the initial top-right initial scenario of the (5, 1)-BOS CA of Fig. 2 with increasing values of the α memory factor. Even the lowest memory charge implemented in the figure ($\alpha = 0.1$) alters the dynamics compared to the ahistoric scenario. Though not qualitatively, the general form of the evolving curves is preserved. This overall rule applies in general provided that memory is not absolute, i.e., $\alpha = 1.0$. Full memory has a fully inhibitory effect in the dynamic, regardless the initial configuration, as shown in Fig. 8 in a particular case. The effect of $\alpha = 0.5$ in Fig. 8 is highly unexpected. To check its exceptionality, the remaining eight initial scenarios of Fig. 2 where run under $\alpha = 0.5$ memory, and a similar abrupt behavior (though not so determinant) was only observed in the case of the 7 initial configuration.

Memory enables the generation of continuous-valued simulations from crisp, i.e., 0 or 1, initial F-degrees. Thus, for example, if the non-1 male player in Table 2 plays $x = 0.0$ instead of 0.5, the F-degree trait of his neighbors at $T = 2$ implementing α memory would be $\chi = \alpha/(1 + \alpha)$. This non-binary value will be that spreaded at $T = 3$. The mean F-degrees and payoffs in simulations with memory starting from random crisp F-degrees evolve much as evolve those starting from F-degrees in the [0, 1] interval. Nevertheless, a higher proximity in the payoffs of both types o players is often achieved. This is so for example in the initial scenario of Fig. 1, in which case both mean payoffs are nearly coincident when $\alpha \geq 0.5$.

4.1 Other Memories

Memory can actuate either only in payoffs, or only in F-degrees. Any kind of these partial memory implementations induces an effect on the dynamics qualitatively similar to that produced when both memory of payoffs and F-degrees actuate together. Thus, for example,

Table 3 The continuous-valued (5, 1)-BOS CA with full memory in the 6×6 scenario of Table 2

$T = 2$

χ, v						$\pi_{♂}, \pi_{♀}$					
1	0	1	0	1	0	0	2.5	0	2.5	0	0
0	.75	0	.75	0	1	2.5	2.0	10	2.0	2.5	0
1	0	.50	0	1	0	0	10	4.0	10	0	0
0	.75	0	.75	0	1	2.5	2.0	10	2.0	2.5	0
1	0	1	0	1	0	0	2.5	0	2.5	0	0
0	1	0	1	0	1	0	0	0	0	0	0

$T = 3$

x, y						$p_{♂}, p_{♀}$					
.75	0	.75	0	.75	0	1.0	5.0	1.0	1.0	5.0	2.5
0	0.5	0	0.5	0	1	5.0	2.0	875	2.0	5.0	0
.75	0	0.5	0	.75	0	1.0	875	2.0	875	1.0	2.5
0	0.5	0	0.5	0	1	5.0	2.0	875	2.0	5.0	0
.75	0	.75	0	.75	0	1.0	5.0	1.0	1.0	5.0	2.5
0	1	0	1	0	1	2.5	0	2.5	0	2.5	0

[4] $\Delta p = p_{♂} - p_{♀} = 4(x + y - 1)$, $L = (6y - 1)x + 1 - y + \lambda(\Delta p - 4(x + y - 1))$, $\frac{\partial L}{\partial x} = 6y - 1 - 4\lambda$, $\frac{\partial L}{\partial y} = 6x - 1 - 4\lambda$, $\max L \to x = y = \frac{1+4\lambda}{6} \to \Delta p = 4(2\frac{1+4\lambda}{6} - 1) \to \lambda = \frac{3\Delta p+8}{16} \to x = y = \frac{\Delta p+4}{8}$, $p_{♂} = 6xy - (x + y) + 1 = 6(\frac{\Delta p+4}{8})^2 - \frac{\Delta p+4}{4} + 1$.

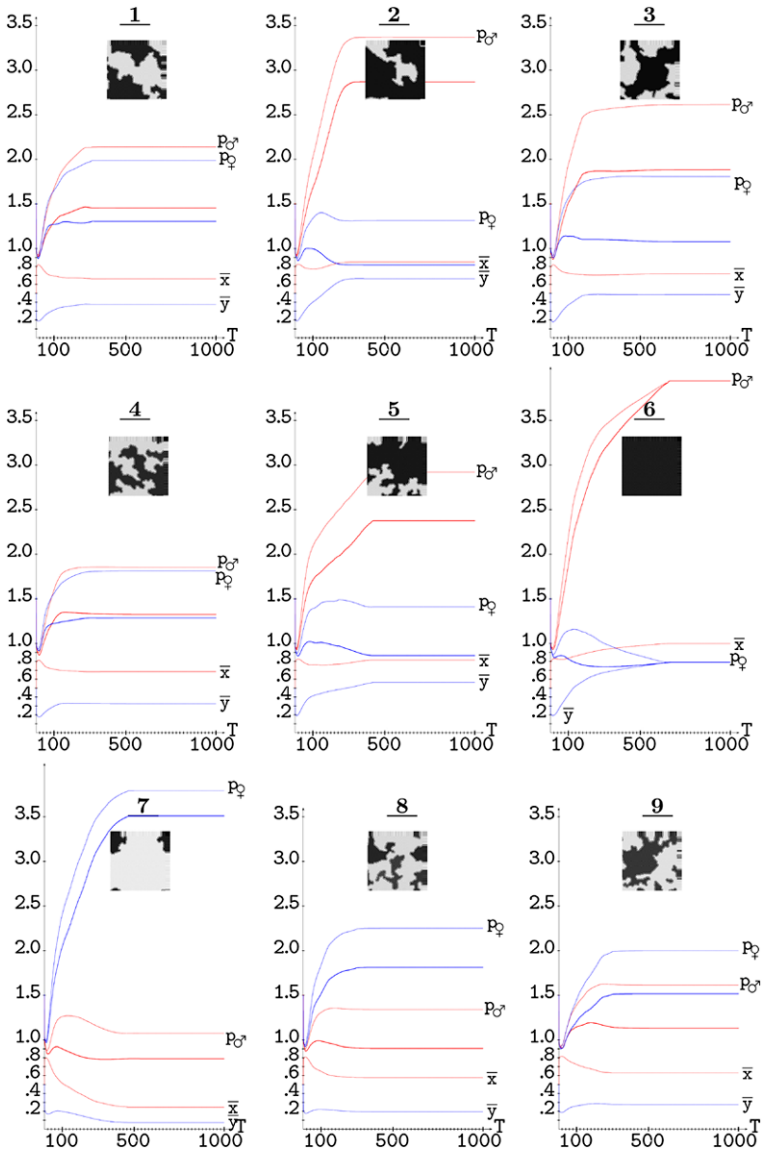

Fig. 7 The F-degrees and mean payoff per encounter ($\mathfrak{P}$) in the nine initial scenarios of the deterministic (5, 1)-BOS CA of Fig. 2 with $\alpha = 0.7$ memory

the evolution of the simulations in the initial contexts of Fig. 8 but with any of the available partial memory implementations (not shown here), is qualitatively similar to that with both p and F-memory. The only apparent difference is the standard behavior with partial memory of the $\alpha = 0.5$ simulation.

Instead of considering unlimited trailing memory as done up to now, the length of the trailing memory can be limited up to the last τ time-steps. Thus, $\pi_i^{(T)} = \pi(p_i^{(T-\tau+1)},$

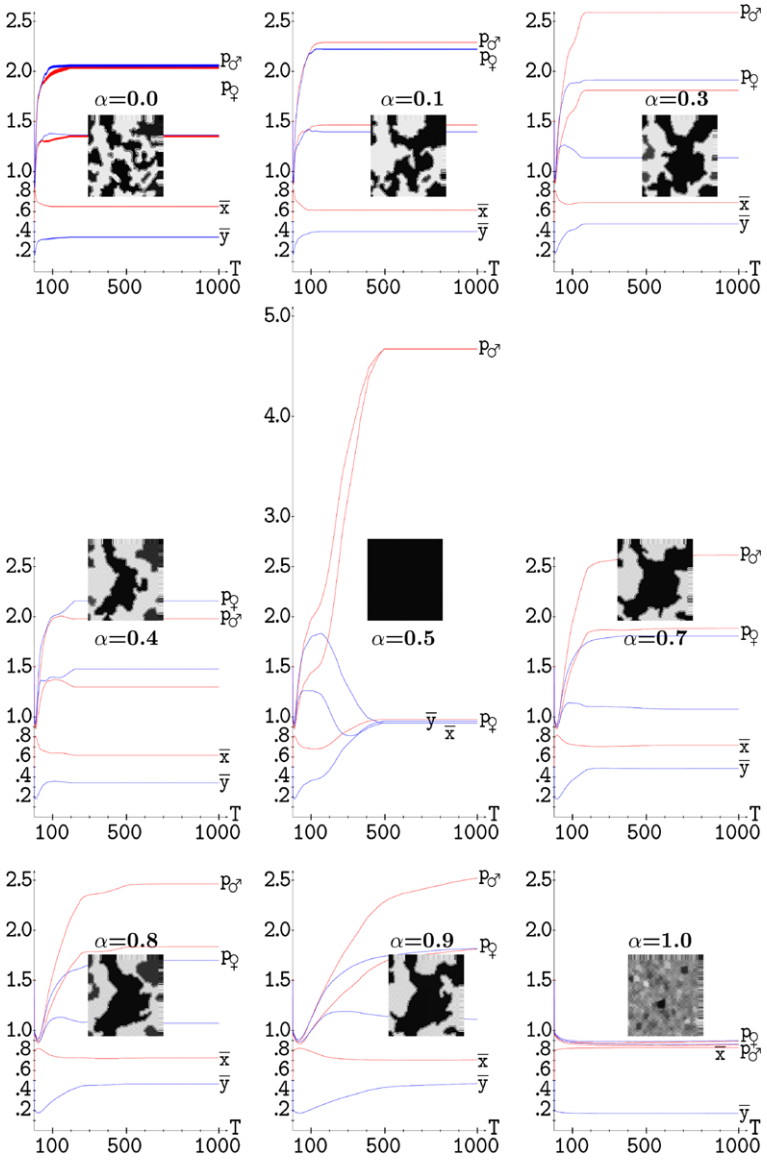

Fig. 8 Dynamics in the initial top-right scenario of Fig. 2 with increasing values of the α memory factor

$\ldots, p_i^{(T)})$, $\begin{matrix}\chi_i^{(T)}=\chi(x_i^{(T-\tau+1)},\ldots,x_i^{(T)})\\ \upsilon_i^{(T)}=\upsilon(y_i^{(T-\tau+1)},\ldots,y_i^{(T)})\end{matrix}$. In the extreme case, $\tau = 1$ leads to the *ahistoric*, rather Markovian, model: $\pi_i^{(T)} = p_i^{(T)}$, $\chi_i^{(T)} = x_i^{(T)}$, $\upsilon_i^{(T)} = y_i^{(T)}$.

As an overall rule, τ-limited trailing memory excerpts effects similar to that of unlimited range memory with low α memory factor. Nevertheless, higher levels of coordination have been frequently found in the nine initial scenarios considered here with $\tau = 3$ limited trailing memory. Thus for example, Fig. 9 shows the evolution up to $T = 1000$ of the F-degree and mean payoff per encounter in the initial top-right scenario of Fig. 2 with $\tau = 3$ memory and

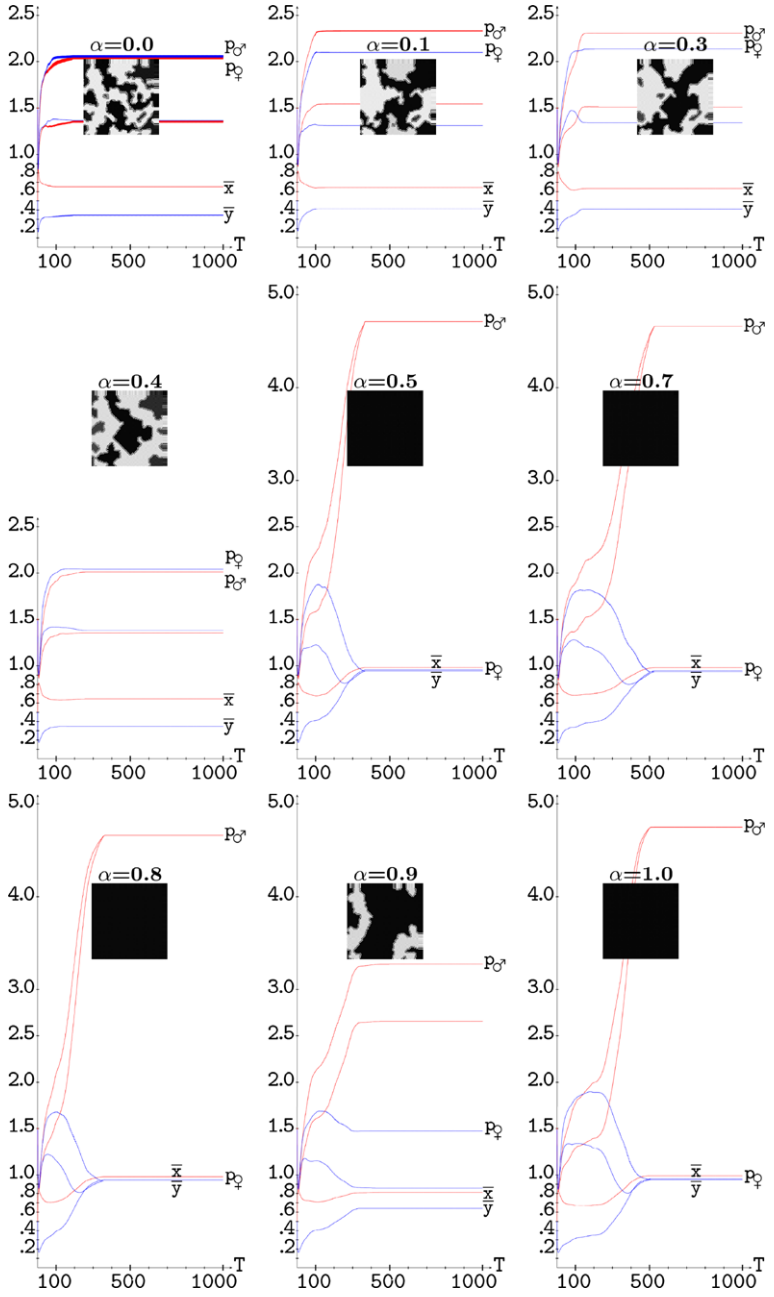

Fig. 9 Dynamics in the initial top-right scenario of Fig. 2 with $\tau = 3$ memory and increasing values of the α memory factor

increasing values of the α memory factor. Short range memory alters the dynamics, though only significantly if $\alpha \geq 0.5$ in Fig. 9, in which case the drift to the $(5, 1)$ steady state is predominant. This scheme is not fully representative of the effect of $\tau = 3$ memory in the

remaining simulations with respect to full coordination, albeit dynamics such as that of $\alpha = 0.9$ in Fig. 9 are not infrequent. The kind of minimal trailing memory, i.e.[5], $\tau = 2$, alters the dynamics much in the way as $\tau = 3$ does, but not in exactly the same way. Thus for example, with $\tau = 2$ memory the simulation in the initial scenario of Fig. 9 (i.e., simulation 3), only converges to the (5, 1) steady state if $\alpha = 0.4$ or $\alpha = 0.5$.

4.2 Probabilistic Updating with Memory

The probabilistic updating scheme becomes with memory

$$P\left(x_i^{(T+1)} = \chi_j^{(T)}\right) = \frac{\pi_j^{(T)}}{\sum_{j\in\mathcal{N}_i} \pi_j^{(T)}}, \qquad P\left(y_i^{(T+1)} = \upsilon_j^{(T)}\right) = \frac{\pi_j^{(T)}}{\sum_{j\in\mathcal{N}_i} \pi_j^{(T)}}. \tag{4}$$

Unlimited trailing memory *freezes* the dynamics in the model with probabilistic updating since the very beginning. Thus, after a weak initial perturbation, the mean F-degrees stabilize near their initial values. This is so even favoring the most successful mate neighbor by means of low levels of the $m > 1$ parameter in

$$P\left(x_i^{(T+1)} = \chi_j^{(T)}\right) = \frac{\pi_j^{(T)^m}}{\sum_{j\in\mathcal{N}_i} \pi_j^{(T)^m}}, \qquad P\left(y_i^{(T+1)} = \upsilon_j^{(T)}\right) = \frac{\pi_j^{(T)^m}}{\sum_{j\in\mathcal{N}_i} \pi_j^{(T)^m}}. \tag{5}$$

In order to avoid arithmetic overflow, the mean payoff across time-steps is preferred to the accumulative payoff in (5). So, $\overline{\pi_i^{(T)}} = \frac{\pi_i^{(T)}}{\Omega(T)}$ instead of $\pi_i^{(T)}$. This allows for the implementation of higher values of m. Thus, $m = 10$ in Fig. 10, in which case the dynamics turns out rather erratic. There are frequent cases of notable proximity between the actual and theoretical payoffs (simulations 1, 4, 5, 6, 7, 9), which indicate the absence of coincidence clusters, as appreciated in the F-degree patterns at $T = 2000$ shown in Fig. 10 as insets.

Limited trailing memory does not excerpt the inhibitory effect on the dynamics with probabilistic updating above mentioned regarding unlimited trailing memory. On the contrary, $\tau = 3$ memory implementations of the simulations in Fig. 4 for example do not significantly alter the dynamics in most cases, and, above all, the predominance of the payoffs of both kind of players is very seldom inverted.

5 Conclusions and Future Work

With deterministic updating, the spatial structure enables the emergence of coordination clusters in the BOS game, leading to the mean payoffs per encounter to values that are accessible only in the cooperative two-person game scenario, which constitutes a notable case of self-organization. With probabilistic updating of choices, both kinds of player tend to reach a full coordination absorbing steady state in the long term. As a general rule, short-term memory of past iterations does not qualitatively alter the ahistoric dynamics, not even in the probabilistic updating scenario. Unlimited trailing memory induces a heavier inertial effect, which alters the dynamics to a larger extent. This is so particularly notable in the

[5] $\pi_i^{(T)} = \alpha p_i^{(T-1)} + p_i^{(T)}$, $\begin{matrix}\chi_i^{(T)}=(\alpha x_i^{(T-1)}+x_i^{(T)})(1+\alpha)\\ \upsilon_i^{(T)}=(\alpha y_i^{(T-1)}+y_i^{(T)})/(1+\alpha)\end{matrix}$.

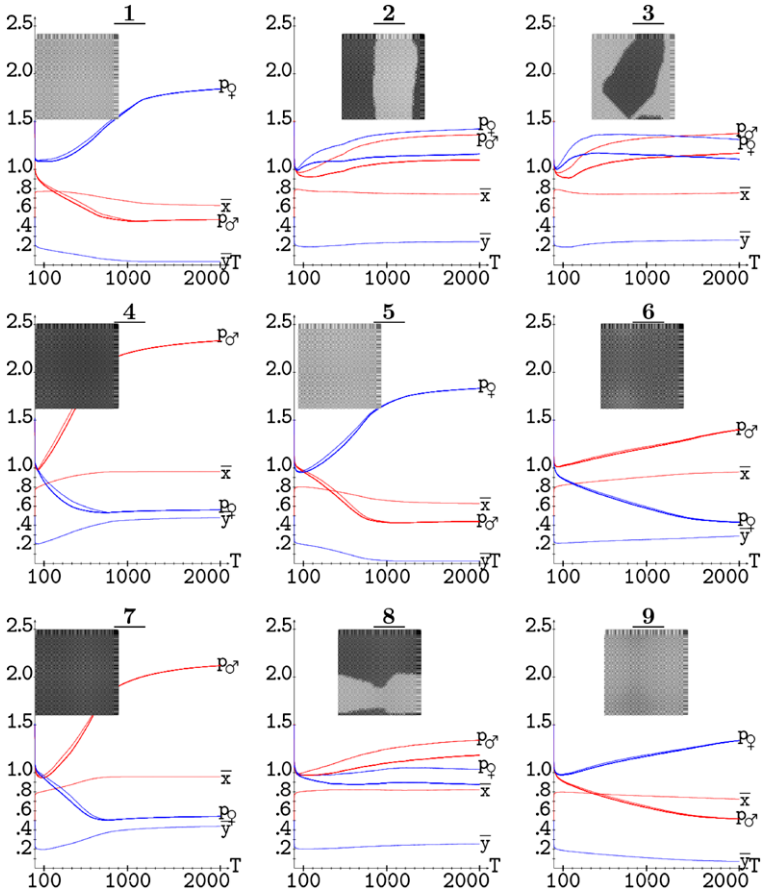

Fig. 10 The F-degrees and mean payoff per encounter (p) in the nine initial scenarios of the (5, 1)-BOS CA of Fig. 2 with $m = 10$ probabilistic updating, and $\alpha = 0.7$ memory

probabilistic updating scenario, in which case unlimited trailing memory fully inhibits the dynamics.

In real-life situations the preferential choice and refusal of partners plays an important role in the emergence of cooperation [22]. We have studied the effect of memory on a simple, deterministic, structurally dynamic PD game, in which state and link configurations are *both* dynamic and are continually interacting [3]. Further study is due on the structurally dynamic battle of the sexes. The study of the effect of memory in other structurally spatialized games, as well as in games on networks [1] is also planned as a future work.

Asynchronous updating, as well as the effect of increasing degrees of spatial dismantling (via rewiring for example, as done in [2] in the PD context), which would lead to more realistic models, are tasks left to be scrutinized in further studies.

Correlation, namely *entanglement*, is in the core of quantum theory, thus in quantum games [10], and consequently in the quantum approach to the battle of the sexes [11, 18]. Last but not least, quantum BOS in the spatialized context is to be studied in the near future.

Acknowledgements This work was carried out during a two-months residence in the University of the West of England (Bristol), supported by EPSRC grant EP/H014381/1.

References

1. Alonso-Sanz R (2009) Spatial order prevails over memory in boosting cooperation in the iterated prisoner's dilemma. Chaos 19(2):023102
2. Alonso-Sanz R (2009) Memory versus spatial disorder in the support of cooperation. Biosytems 97:90–102
3. Alonso-Sanz R (2009) Memory boosts cooperation in the structurally dynamic prisoner's dilemma. Int J Bifurc Chaos 19(9):2899–2926
4. Alonso-Sanz R (2011) Self-organization in the battle of the sexes. Int J Mod Phys C 22(1):1–11
5. Alonso-Sanz R (2011) Self-organization in spatial battle of the sexes with probabilistic updating. Physica A 390:2956–2967
6. Alonso-Sanz R, Martin M (2005) Memory boosts cooperation. Int J Mod Phys C 17(6):841–852
7. Alonso-Sanz R, Martin MC, Martin M (2001) The effect of memory in the spatial continuous-valued prisoner's dilemma. Int J Bifurc Chaos 11(8):2061–2083, and the references therein
8. Aumann RJ (1987) Correlated equilibrium as an expression of Bayesian rationality. Econometrica 55(1):1–18
9. Axelrod R (2008) The evolution of cooperation, revised edn. Basic Books, New York
10. Eisert J, Wilkens M, Lewenstein M (1999) Quantum games and quantum strategies. Phys Rev Lett 83(15):3077–3080
11. Frackiewicz P (2009) The ultimate solution to the quantum battle of the sexes game. J Phys A, Math Gen 42(36):365305
12. Hauert C, Schuster HG (1997) Effect of increasing the number of players and memory steps in the iterated prisoner's dilemma, a numerical approach. Proc R Soc Lond B 264:513
13. Hofbauer J, Sigmund K (2003) Evolutionary games and population dynamics. Cambridge University Press, Cambridge
14. Lindgren K, Nordahl MG (1994) Evolutionary dynamics of spatial games. Physica D 75:292–309
15. Lindgren K, Nordahl MG (1995) Cooperation and community structure in artificial ecosystems. In: Langton C (ed) Artificial life. MIT Press, Cambridge, pp 16–37
16. Luce RD, Raiffa H (1989) Games and decisions: introduction and critical survey. Dover, New York
17. Maynard Smith J (1982) Evolution and the theory of games. Cambridge University Press, Cambridge
18. Nawaz A, Toor AH (2004) Dilemma and quantum battle of sexes. J Phys A, Math Gen 37(15):4437–4443
19. Nowak NM, May RM (1992) Evolutionary games and spatial chaos. Nature 359:826–829
20. Nowak MA, May M (1993) The spatial dilemmas of evolution. Int J Bifurc Chaos 3(11):35–78
21. Owen G (1995) Game theory. Academic Press, New York
22. Szabo G, Fáth G (2007) Evolutionary games on graphs. Phys Rep 446:97–216
23. Zhao J, Szilagyi N, Szidarovsky F (2008) An n-person battle of sexes game. Physica A 387:3669–3677
24. Zhao J, Szilagyi N, Szidarovsky F (2008) An n-person battle of sexes game—a simulation study. Physica A 387:3668–3788